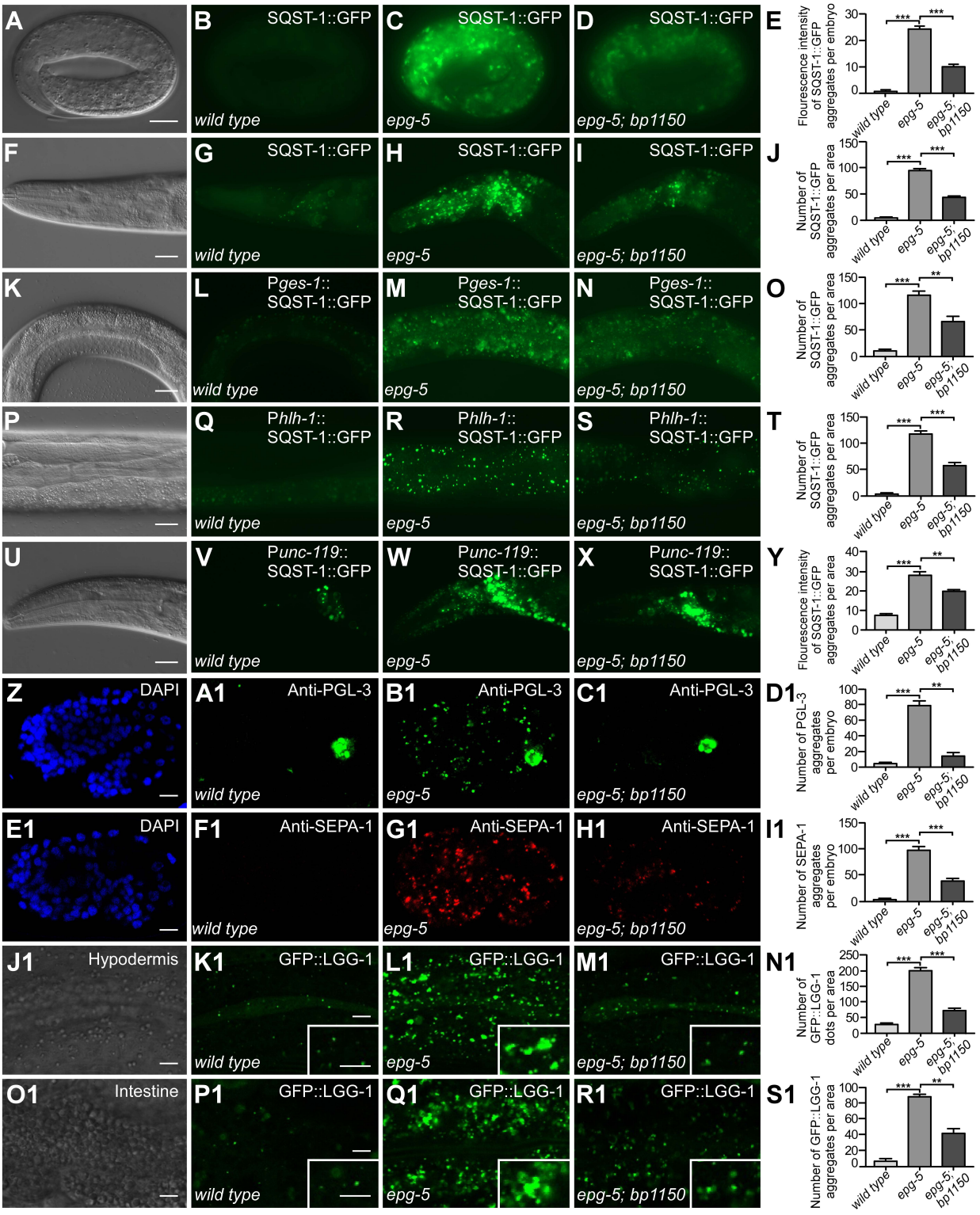

Figure S1

Figure S1. *bp1150* suppresses the autophagy defect in *epg-5* mutants.

(A-E) SQST-1::GFP is weakly expressed and diffusely localized in wild-type embryos (B). (A) shows the differential interference contrast (DIC) image of the embryo in (B). SQST-1::GFP accumulates into a large number of aggregates in *epg-5* mutants (C). In *epg-5; bp1150* double mutants, the accumulation of SQST-1::GFP is weaker than in *epg-5* animals (D). 4-fold stage embryos are shown in (A-D). (E) shows quantification of the fluorescence intensity of SQST-1::GFP in wild-type, *epg-5* and *epg-5; bp1150* embryos. Data are shown as mean ± S.E.M. (n=7). ***p<0.001. Scale bar: 10 μm (A-D).

(F-J) SQST-1::GFP forms only a few small aggregates in the head region in wild-type animals (G). (F) shows the DIC image of the animal in (G). A large number of SQST-1::GFP aggregates accumulate in *epg-5* mutants (H). In *epg-5; bp1150* double mutants, the number of SQST-1::GFP aggregates is less than in *epg-5* animals (I). Quantification of the number of SQST-1 in wild type, *epg-5* mutants and *epg-5; bp1150* mutants is shown as mean ± S.E.M. (n=8) in (J). “Area” used for quantification refers to the captured image. ***p<0.001. Scale bar: 20 μm (F-I).

(K-O) In wild-type animals, SQST-1::GFP does not accumulate when expressed specifically in intestine (L). (K) shows the DIC image of the animal in (L). In *epg-5* mutants, SQST-1::GFP accumulates into numerous aggregates (M) and the number is dramatically reduced by the *bp1150* mutation (N). The faint GFP

puncta in the background are intestinal autofluorescence (N). Quantification of the number of SQST-1::GFP puncta in wild type, *epg-5* mutants and *epg-5; bp1150* mutants is shown as mean ± S.E.M. (n=5) in (O). **p<0.01, ***p<0.001. Scale bar: 20 μm (K-N).

(P-T) In wild-type animals, SQST-1::GFP forms a few small aggregates when specifically expressed in muscle (Q). (P) shows the DIC image of the animal in (Q). Numerous SQST-1::GFP aggregates accumulate in *epg-5* mutants (R). In *epg-5; bp1150* double mutants, the number of SQST-1::GFP dots is much less than in *epg-5* animals (S). Quantification of the number of SQST-1::GFP aggregates in wild type, *epg-5* mutants and *epg-5; bp1150* mutants is shown as mean ± S.E.M. (n=8) in (T). ***p<0.001. Scale bar: 20 μm (P-S).

(U-Y) SQST-1::GFP driven by the neuronal-specific promoter *unc-119* forms a few aggregates in the head region in wild-type animals (V). (U) is the DIC image of the animal shown in (V). In *epg-5* mutants, SQST-1::GFP accumulates into a large number of aggregates (W), and this is ameliorated by *bp1150* (X). (Y) shows quantification of the fluorescence intensity of SQST-1::GFP in wild type, *epg-5* mutants and *epg-5; bp1150* mutants. Data are shown as mean ± S.E.M. (n=5). **p<0.01, ***p<0.001. Scale bar: 20 μm (U-X).

(Z-D1) PGL granules, detected by anti-PGL-3 antibody (diluted 1:1000), are absent in somatic cells in wild-type embryos at the comma stage (A1). PGL-3-labeled granules are present in germline precursor cells Z2 and Z3. (Z) shows the DAPI image of the embryo in (A1). PGL-3 granules dramatically accumulate in somatic

cells in *epg-5* mutant embryos (B1). Accumulation of PGL granules is suppressed in *epg-5; bp1150* embryos (C1). Quantification of the number of PGL granules in somatic cells in wild type, *epg-5* mutants and *epg-5; bp1150* mutants is shown as mean ± S.E.M. (n=3) in (D1). **p<0.01, ***p<0.001. Scale bar: 5 μm (Z-C1).

(E1-I1) SEPA-1 aggregates, detected by anti-SEPA-1 antibody (diluted 1:10000), are absent in comma stage wild-type embryos (F1). (E1) shows the DAPI image of the embryo in (F1). A large number of SEPA-1 aggregates accumulate in *epg-5* mutant embryos at the comma stage (G1), and this is dramatically suppressed in *epg-5; bp1150* embryos (H1). Quantification of the number of SEPA-1 aggregates in wild type, *epg-5* mutants and *epg-5; bp1150* mutants is shown as mean ± S.E.M. (n=4) in (I1). ***p<0.001. Scale bar: 5 μm (E1-H1).

(J1-N1) Expression of GFP::LGG-1 in the hypodermis of wild-type, *epg-5* and *epg-5; bp1150* animals. In wild-type hypodermis, GFP::LGG-1 is weakly expressed and forms a few small puncta (K1). (J1) shows the DIC image of the animal in (K1). A large number of GFP::LGG-1 puncta accumulate in *epg-5* mutants (L1) and the number is decreased in *epg-5; bp1150* double mutants (M1). Quantification of the number of GFP::LGG-1 in wild type, *epg-5* mutants and *epg-5; bp1150* mutants is shown as mean ± S.E.M. (n=5) in (N1). ***p<0.001. Scale bar: 5 μm (J1-M1).

(O1-S1) Expression of GFP::LGG-1 in wild-type, *epg-5* and *epg-5; bp1150* intestine. In wild-type intestine, GFP::LGG-1 is weakly expressed and forms a few small puncta (P1). (O1) shows the DIC image of the animal in (P1). Numerous GFP::LGG-1 puncta accumulate in *epg-5* mutant intestine (Q1). The number of

GFP::LGG-1 puncta is decreased in *epg-5; bp1150* double mutants (R1).

Quantification of the number of GFP::LGG-1 in wild type, *epg-5* mutants and *epg-5; bp1150* mutants is shown as mean ± S.E.M. (n=5) in (S1). **p<0.01, ***p<0.001. Scale bar: 5 μm (O1-R1).

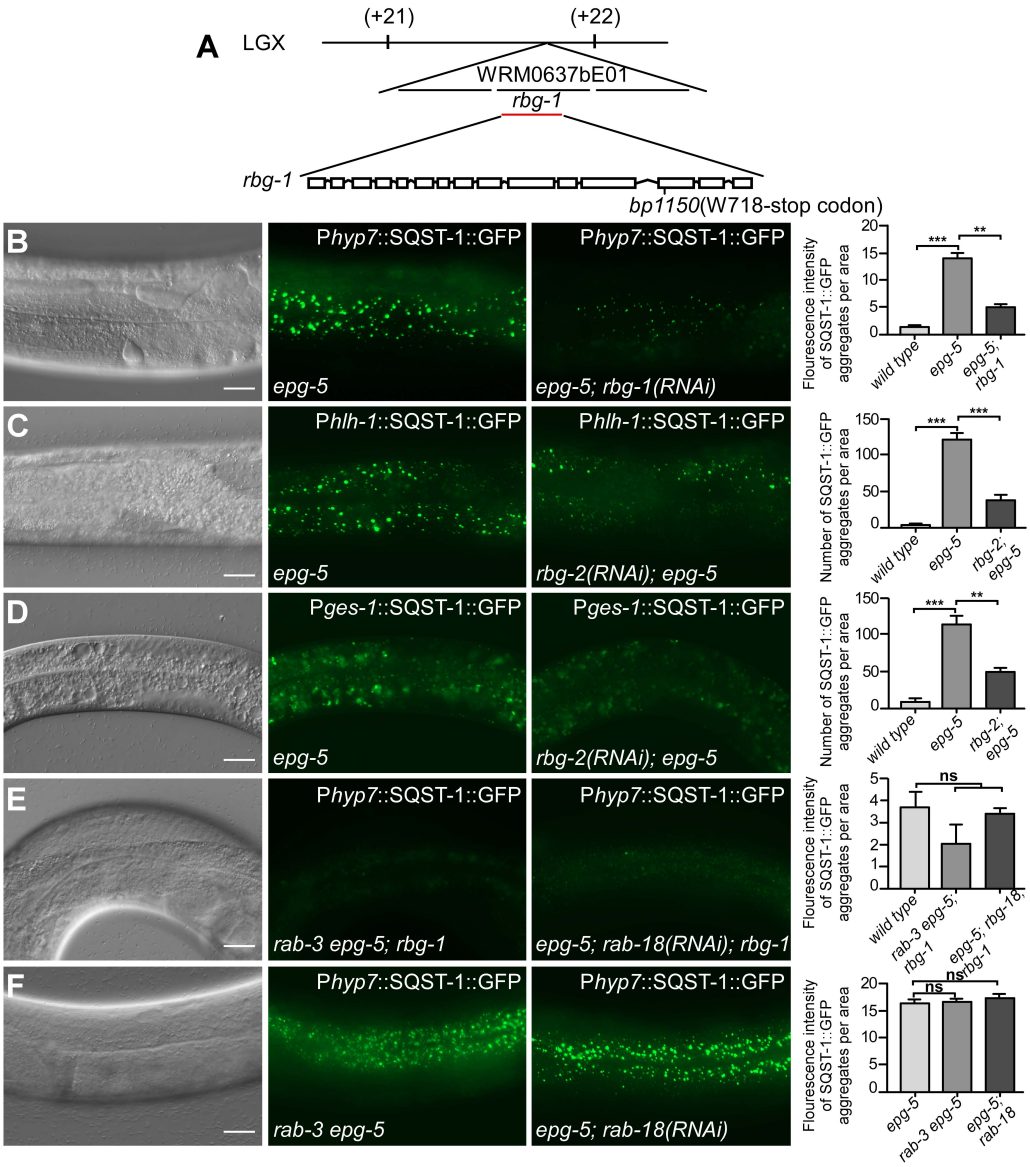

Figure S2

Figure S2. The RBG-1/RBG-2 complex modulates degradation of SQST-1 aggregates in *epg-5* mutants in a manner independent of RAB-3 and RAB-18.

(A) A transgene expressing *rbg-1* rescues the phenotype in *bp1150* mutants. *bp1150* contains a tryptophan to stop codon mutation at residue 718 in RBG-1.

(B) *rbg-1(RNAi)* suppresses the accumulation of SQST-1::GFP aggregates in *epg-5* mutants. SQST-1::GFP is specifically expressed in the hypodermis. Quantification of the fluorescence intensity of SQST-1::GFP in various genetic backgrounds is shown as mean ± S.E.M. (n=8). **p<0.01, ***p<0.001.

(C,D) Accumulation of SQST-1::GFP aggregates in *epg-5* muscles (C) and the intestine (D) is suppressed by simultaneous depletion of *rbg-2*. SQST-1::GFP is driven by a tissue-specific promoter. The faint GFP puncta in the background are intestinal autofluorescence (D). Quantification of the number of SQST-1::GFP aggregates in various genetic backgrounds is shown as mean ± S.E.M. (n=6). **p<0.01, ***p<0.001.

(E) Loss of function of *rab-3* and *rab-18* fail to restore the accumulation of SQST-1::GFP aggregates in the *epg-5; rbg-1* hypodermis. Quantification of the fluorescence intensity of SQST-1::GFP in various genetic backgrounds is shown as mean ± S.E.M. (n=6). ns: no significant difference.

(F) Loss of function of *rab-3* and *rab-18* fail to suppress the accumulation of SQST-1::GFP aggregates in *epg-5* hypodermal cells. Quantification of the fluorescence intensity of SQST-1::GFP in various genetic backgrounds is shown as mean ± S.E.M. (n=5). ns: no significant difference. Scale bar: 20 μm (B-F).

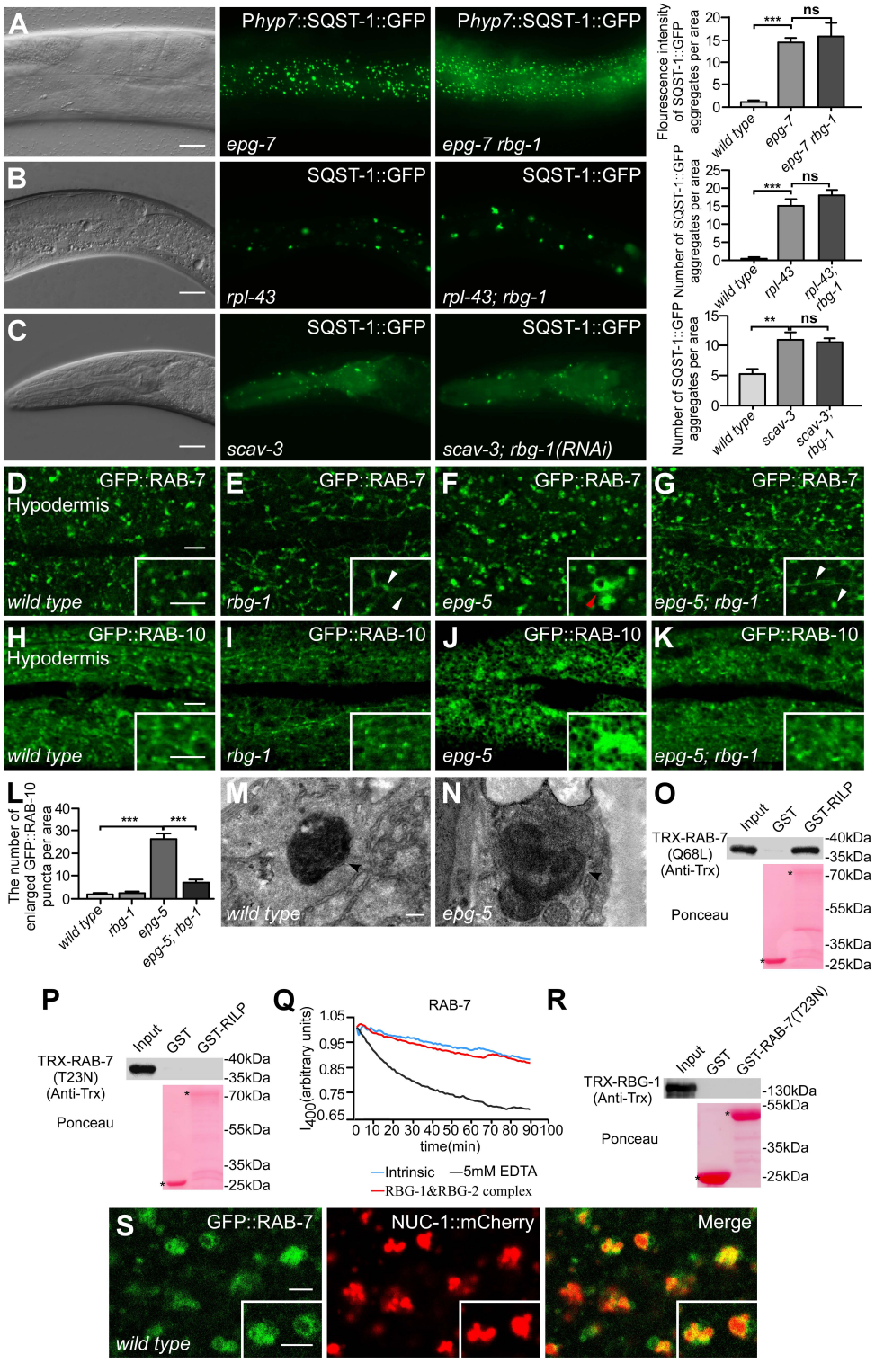

Figure S3

Figure S3. Loss of *rbg-1* activity suppresses the autophagy defect in *epg-5* mutants but does not generally elevate autophagy activity.

(A) In *epg-7* hypodermis, a large number of SQST-1::GFP aggregates accumulate, and this is slightly increased by loss of function of *rbg-1*, although the change is not statistically significant. Quantification of the fluorescence intensity of SQST-1::GFP in various genetic backgrounds is shown as mean ± S.E.M. (n=5). ***p<0.001, ns: no significant difference. Scale bar: 20 μm (A).

(B) In *rpl-43* intestine, SQST-1::GFP accumulates into large aggregates, and this can be suppressed by elevating autophagy activity (Guo et al., 2014), but not by simultaneous loss of function of *rbg-1*. Quantification of the number of SQST-1::GFP aggregates in the indicated genetic backgrounds is shown as mean ± S.E.M. (n=5). ***p<0.001, ns: no significant difference. Scale bar: 20 μm (B).

(C) A few SQST-1::GFP aggregates accumulate in *scav-3* mutants, and this is not affected by loss of *rbg-1* activity. Quantification of the number of SQST-1::GFP aggregates in the indicated genetic backgrounds is shown as mean ± S.E.M. (n=6). **p<0.01. ns: no significant difference. Scale bar: 20 μm (C).

(D-G) GFP::RAB-7 labels spherical structures and a few tubular structures in wild-type animals (D). *rbg-1* mutants contain more GFP::RAB-7-labeled small spherical structures and tubular structures than wild-type worms (E). GFP::RAB-7 labels enlarged ring-like structures and shows no tubular structures in *epg-5* mutants (F). In *epg-5; rbg-1* double mutants, the abnormally enlarged

GFP::RAB-7-labeled structures are suppressed (G). White arrowheads indicate the small spherical and tubular structures. Red arrowhead indicates the abnormal ring-like structure in *epg-5* mutants. Scale bar: 5 μm (D-G).

(H-K) GFP::RAB-10 forms small dots in the hypodermis in wild-type (H) and *rbg-1* animals (I), while it forms abnormally big puncta in *epg-5* mutants (J). The formation of enlarged GFP::RAB-10 puncta is suppressed in *epg-5; rbg-1* double mutants (K). Scale bar: 5 μm (H-K).

(L) Quantification of enlarged GFP::RAB-10 puncta in wild-type, *rbg-1*, *epg-5* and *epg-5; rbg-1* animals. Data are shown as mean ± S.E.M. (n=5). ***p<0.001.

(M,N) Electron microscopy analysis reveals that compared to wild-type animals, *epg-5* mutants contain enlarged lysosomal structures with abnormal appearance. Arrowheads indicate the lysosomal structures. Scale bar: 200 nm (M,N).

(O) In an *in vitro* GST pulldown assay, TRX-RAB-7(Q68L) is specifically pulled down by GST-RILP.

(P) In an *in vitro* GST pulldown assay, TRX-RAB-7(T23N) fails to be pulled down by GST-RILP.

(Q) The RBG-1/RBG-2 complex does not possess evident GEF activity towards RAB-7.

(R) In an *in vitro* GST pulldown assay, TRX-RBG-1 fails to be pulled down by GST-RAB-7(T23N).

(S) GFP::RAB-7 forms ring-like structures that enclose the lysosomal-localized DNase II NUC-1::mCherry. Scale bar: 0.25 μm.

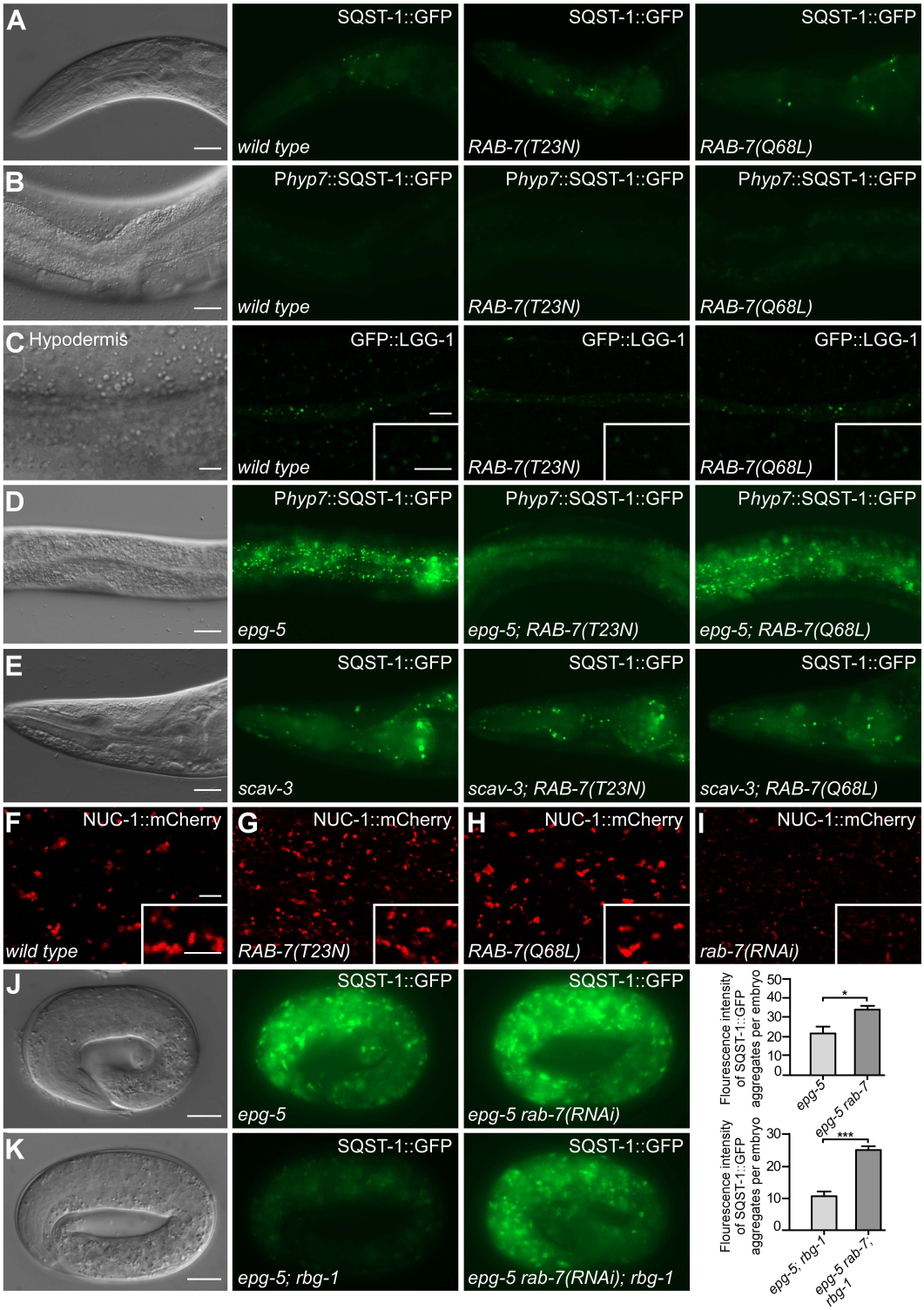

Figure S4

Figure S4. Expression of RAB-7(T23N), but not RAB-7(Q68L) or *rab-7(RNAi)*, mimics the effect of loss of function of *rbg-1* on autophagy.

(A-C) In animals expressing RAB-7(T23N) and RAB-7(Q68L), SQST-1::GFP (A, B) and GFP::LGG-1(C) show no evident accumulation. Scale bar: 20 μm (A, B); 5 μm (C).

(D) The accumulation of SQST-1::GFP aggregates in *epg-5* hypodermis is suppressed by expression of RAB-7(T23N), but not by RAB-7(Q68L). Scale bar: 20 μm (D).

(E) The accumulation of SQST-1::GFP aggregates in *scav-3* mutants is not suppressed by expression of RAB-7(T23N) and RAB-7(Q68L). Scale bar: 20 μm (E).

(F-I) Compared to wild-type animals, the NUC-1::mCherry-labeled lysosomes are smaller in animals expressing RAB-7(T23N) (G), but show no change in RAB-7(Q68L)-expressing animals (H). NUC-1::mCherry labels many tiny dots in *rab-7(RNAi)* animals (I). Scale bar: 5 μm (F-I).

(J,K) *RNAi* inactivation of *rab-7* enhances the accumulation of SQST-1::GFP aggregates in *epg-5* (J) and *epg-5; rbg-1* (K) embryos. Quantification of the fluorescence intensity of SQST-1::GFP in various genetic backgrounds is shown as mean ± S.E.M. (n=5). *p<0.05, ***p<0.001. Scale bar: 10 μm (J,K).

Table S1. *C. elegans* strains used in this work.

Strain	Genotype	Source
FX03425	*epg-5(tm3425)*	From Dr. Shohei Mitani
HZ3195	*rbg-1(bp1150)*	This work
HZ3524	*epg-5(tm3425); rbg-1(bp1150)*	This work
HZ2043	*bpIs267(P_{hyp-7}SQST-1::GFP, unc-76)*	From Dr. Hong Zhang's lab
HZ4661	*epg-5(tm3425); bpIs267(P_{hyp-7}SQST-1::GFP, unc-76)*	This work
HZ3703	*epg-5(tm3425); rbg-1(bp1150); bpIs267(P_{hyp-7}SQST-1::GFP, unc-76)*	This work
HZ1528	*bpIs151(P_{sqst-1}SQST-1::GFP, unc-76)*	From Dr. Hong Zhang's lab
HZ3716	*epg-5(tm3425); bpIs151(P_{sqst-1}SQST-1::GFP, unc-76)*	This work
HZ3516	*epg-5(tm3425); rbg-1(bp1150); bpIs151(P_{sqst-1}SQST-1::GFP, unc-76)*	This work
HZ2038	*bpIs262(P_{ges-1}SQST-1::GFP, unc-76)*	From Dr. Hong Zhang's lab
HZ3701	*epg-5(tm3425); bpIs262(P_{ges-1}SQST-1::GFP, unc-76)*	This work
HZ3479	*epg-5(tm3425); rbg-1(bp1150); bpIs262(P_{ges-1}SQST-1::GFP, unc-76)*	This work
HZ4249	*bpIs193(P_{hlh-1}SQST-1::GFP, unc-76)*	From Dr. Hong Zhang's lab
HZ3728	*epg-5(tm3425); bpIs193(P_{hlh-1}SQST-1::GFP, unc-76)*	This work
HZ3713	*epg-5(tm3425); rbg-1(bp1150); bpIs193(P_{hlh-1}SQST-1::GFP, unc-76)*	This work
HZ2780	*bpIs328($P_{unc-119}$SQST-1::GFP, Pord-1::RFP)*	From Dr. Hong Zhang's lab
HZ4651	*epg-5(tm3425); bpIs328($P_{unc-119}$SQST-1::GFP, Pord-1::RFP)*	This work
HZ4653	*epg-5(tm3425); rbg-1(bp1150); bpIs328($P_{unc-119}$SQST-1::GFP, Pord-1::RFP)*	This work
DA2123	*adIs2122(P_{lgg-1}GFP::LGG-1, rol-6(su1006))*	CGC
HZ3486	*epg-5(tm3425); adIs2122(P_{lgg-1}GFP::LGG-1, rol-6(su1006))*	This work
HZ3519	*rbg-1(bp1150); adIs2122(P_{lgg-1}GFP::LGG-1, rol-6(su1006))*	This work
HZ3488	*epg-5(tm3425); rbg-1(bp1150); adIs2122(P_{lgg-1}GFP::LGG-1, rol-6(su1006))*	This work
HZ4660	*rab-3(bp1558) epg-5(tm3425); bpIs267(P_{hyp-7}SQST-1::GFP, unc-76)*	This work
HZ3193	*rab-3(bp1558) epg-5(tm3425); rbg-1(bp1150); bpIs267(P_{hyp-7}SQST-1::GFP, unc-76)*	This work
HZ3730	*bec-1(bp613); bpIs151(P_{sqst-1}SQST-1::GFP, unc-76)*	From Dr. Hong Zhang's lab
HZ3731	*bec-1(bp613); rbg-1(bp1150); bpIs151(P_{sqst-1}SQST-1::GFP, unc-76)*	This work
HZ3708	*cpl-1(qx304); bpIs151(P_{sqst-1}SQST-1::GFP, unc-76)*	This work
HZ3742	*cpl-1(qx304); rbg-1(bp1150); bpIs151(P_{sqst-1}SQST-1::GFP, unc-76)*	This work
HZ3704	*epg-7(tm2508); bpIs267(P_{hyp-7}SQST-1::GFP, unc-76)*	From Dr. Hong Zhang's lab
HZ3518	*epg-7(tm2508); rbg-1(bp1150); bpIs267(P_{hyp-7}SQST-1::GFP, unc-76)*	This work
HZ946	*rpl-43(bp399); bpIs151(P_{sqst-1}SQST-1::GFP, unc-76)*	From Dr. Hong Zhang's lab

XW8738	*scav-3(qx193); bpIs151(P_{sqst-1}SQST-1::GFP, unc-76)*	From Dr. Xiaochen Wang's lab
XW5399	*qxIs257(P_{ced-1}NUC-1::mCherry, unc-76)*	From Dr. Xiaochen Wang's lab
HZ3475	*epg-5(tm3425); qxIs257(P_{ced-1}NUC-1::mCherry, unc-76)*	This work
HZ4654	*rbg-1(bp1150); qxIs257(P_{ced-1}NUC-1::mCherry, unc-76)*	This work
HZ3480	*epg-5(tm3425); rbg-1(bp1150); qxIs257(P_{ced-1}NUC-1::mCherry, unc-76)*	This work
HZ2215	*qxIs257(P_{ced-1}NUC-1::mCherry, unc-76); qxIs66(P_{ced-1}GFP::RAB-7, unc-76)*	This work
XW19131	*qxIs750(P_{hsp}NUC-1::pHTomato, Pord-1::GFP)*	From Dr. Xiaochen Wang's lab
HZ4655	*epg-5(tm3425); qxIs750(P_{hsp}NUC-1::pHTomato, Pord-1::GFP)*	This work
HZ4656	*rbg-1(bp1150); qxIs750(P_{hsp}NUC-1::pHTomato, Pord-1::GFP)*	This work
HZ4657	*epg-5(tm3425); rbg-1(bp1150); qxIs750(P_{hsp}NUC-1::pHTomato, Pord-1::GFP)*	This work
XW1235	*qxIs66(P_{ced-1}GFP::RAB-7, unc-76)*	From Dr. Xiaochen Wang's lab
HZ3483	*epg-5(tm3425); qxIs66(P_{ced-1}GFP::RAB-7, unc-76)*	This work
HZ3484	*rbg-1(bp1150); qxIs66(P_{ced-1}GFP::RAB-7, unc-76)*	This work
HZ3485	*epg-5(tm3425); rbg-1(bp1150); qxIs66(P_{ced-1}GFP::RAB-7, unc-76)*	This work
XW13734	*qxIs612(P_{hsp}NUC-1::sfGFP::mCherry, unc-76)*	From Dr. Xiaochen Wang's lab
HZ3709	*epg-5(tm3425); qxIs612(P_{hsp}NUC-1::sfGFP::mCherry, unc-76)*	This work
HZ3732	*rbg-1(bp1150); qxIs612(P_{hsp}NUC-1::sfGFP::mCherry, unc-76)*	This work
HZ3743	*epg-5(tm3425); rbg-1(bp1150); qxIs612(P_{hsp}NUC-1::sfGFP::mCherry, unc-76)*	This work
XW17602	*qxIs686(P_{hyp-7}GFP::RAB-10, unc-76)*	From Dr. Xiaochen Wang's lab
HZ4493	*qxIs257(P_{ced-1}NUC-1::mCherry, unc-76); qxIs686(P_{hyp-7}GFP::RAB-10, unc-76)*	This work
HZ4616	*epg-5(tm3425); qxIs257(P_{ced-1}NUC-1::mCherry, unc-76); qxIs686(P_{hyp-7}GFP::RAB-10, unc-76)*	This work
HZ4659	*rbg-1(bp1150); qxIs257(P_{ced-1}NUC-1::mCherry, unc-76); qxIs686(P_{hyp-7}GFP::RAB-10, unc-76)*	This work
HZ4617	*epg-5(tm3425); rbg-1(bp1150); qxIs257(P_{ced-1}NUC-1::mCherry, unc-76); qxIs686(P_{hyp-7}GFP::RAB-10, unc-76)*	This work
HZ4494	*bpEx342(P_{hyp-7}BFP::LGG-1, Pmyo-2::GFP)*	This work
HZ4491	*bpIs395(P_{nfya-1}RAB-7(T23N), rol-6(su1006))*	This work